PERGAMON

International Journal of Heat and Mass Transfer 42 (1999) 1689–1706

International Journal of
HEAT and MASS TRANSFER

Buoyancy driven instability in a horizontal layer of electrically conducting fluid in the presence of a vertical magnetic field

M. Takashima*, M. Hirasawa, H. Nozaki

Department of Physics, Osaka City University, Osaka 558, Japan

Received 5 September 1997; in final form 3 July 1998

Abstract

Linear stability theory is applied to the problem of the onset of buoyancy driven instability in a horizontal layer of electrically conducting fluid heated from below in the presence of a vertical magnetic field. Under the proper boundary conditions on the magnetic field perturbations, the Chebyshev collocation method is adopted to obtain the eigenvalue equation, which is then solved numerically. The critical Rayleigh number R_c, the critical wavenumber a_c and the critical frequency ω_c are obtained for wide ranges of the Prandtl number P_r, the magnetic Prandtl number P_m and the Chandrasekhar number Q. A necessary and sufficient condition for overstability to occur is also obtained. © 1998 Elsevier Science Ltd. All rights reserved.

Nomenclature

a $=(a_x^2+a_y^2)^{1/2}$, wavenumber
a_n, b_n, c_n expansion coefficients defined by equations (53)–(55)
b dimensionless magnetic induction in the z-direction, see equation (25)
$\tilde{b}$ dimensionless magnetic induction in the z-direction in the outer regions, see equation (25)
$\mathbf{B}$ $=(B_x, B_y, B_z)$, magnetic induction
$\tilde{\mathbf{B}}$ $=(\tilde{B}_x, \tilde{B}_y, \tilde{B}_z)$, magnetic induction in the outer regions
B_0 external magnetic induction in the z-direction
c specific heat
C_1, C_2 arbitrary constants
d depth of the fluid layer
D $=\mathrm{d}/\mathrm{d}z$
$\mathbf{E}$ matrix defined by equation (60)
$\mathbf{F}$ matrix defined by equation (60)
$\mathbf{g}$ $=(0, 0, -g)$, gravitational acceleration
k thermal conductivity
N number of terms in the expansions (53)–(55)
p pressure
p_0 pressure at $z=0$
P_m $=\nu/\nu_m$, magnetic Prandtl number
P_r $=\nu/\kappa$, Prandtl number
Q $=B_0^2 d^2\sigma/\rho_0\nu$, Chandrasekhar number
Q^* value of Q at the point of transition from stationary to oscillatory mode
R $=\alpha\beta g d^4/\nu\kappa$, Rayleigh number
t time
t^* dimensionless time, see equation (25)
T temperature
T_0 temperature at the lower boundary
T_1 temperature at the upper boundary
$T_n(\xi)$ Chebyshev polynomial
v dimensionless velocity in the z-direction, see equation (25)
$\mathbf{v}$ $=(v_x, v_y, v_z)$, velocity
x, y, z Cartesian coordinates
x^*, y^*, z^* dimensionless Cartesian coordinates, see equation (25)
$\mathbf{X}$ vector defined by equation (61).

Greek symbols
α coefficient of volume expansion
β $=(T_0-T_1)/d$, adverse temperature gradient
ε $=\tilde{\mu}/\mu$, ratio of magnetic permeabilities
η dynamic viscosity
θ dimensionless temperature, see equation (25)

* Corresponding author

PII: S0017–9310(98)00278–6

κ $=k/\rho_0 c$, thermometric conductivity
λ (complex) time constant
μ magnetic permeability
$\tilde{\mu}$ magnetic permeability in the outer regions
ν $=\eta/\rho_0$, kinematic viscosity
ν_m $=1/\sigma\mu$, magnetic viscosity
ξ variable defined by equation (46)
ξ_m collocation points defined by equation (59)
ρ density
ρ_0 density at $T = T_0$
σ electrical conductivity
Φ, Θ, Ψ, $\tilde{\Psi}$ defined by equation (33)
Φ_n, Θ_n, Ψ_n trial functions defined by equations (53)–(55).
ω frequency (imaginary part of λ).

Subscript
c critical.

Superscripts
n neutral
O oscillatory
S stationary
$^{-}$ (overbar) steady solutions
$'$ (prime) perturbed quantities
$\hat{}$ (hat) defined by equation (47).

1. Introduction

The effect of a vertical magnetic field on buoyancy driven instability in a horizontal layer of electrically conducting, viscous fluid heated from below was first analyzed by Chandrasekhar [1]. He obtained the critical Rayleigh number and the critical wavenumber for the onset of stationary convection as functions of Q (the square of the Hartmann number) in the following three cases (1) both bounding surfaces free, (2) one bounding surface free and the other rigid and (3) both bounding surfaces rigid. For the onset of overstability, however, his analysis was limited to the case when both bounding surfaces are free and, moreover, his boundary conditions on the magnetic field perturbations were not correct. Under these circumstances, he concluded that if $P_r > P_m$, the principle of the exchange of stabilities is valid (i.e., the instability sets in as stationary convection) and, therefore, a necessary condition for overstability to be possible is $P_r < P_m$, where P_r is the Prandtl number and P_m is the magnetic Prandtl number.

The analysis by Chandrasekhar has subsequently been re-examined by several workers. Using the correct boundary conditions on the magnetic field perturbations, Gibson [2] showed that overstability is the preferred state for sufficiently large Q if $P_r < P_m$. Sherman and Ostrach [3] showed that a sufficient condition which will establish the exchange principle is $P_r > P_m$ when Q is very large. Gupta et al. [4] and Banerjee et al. [5] demonstrated that if $QP_m \leqslant \pi^2$, the principle of the exchange of stabilities is valid. Kumar et al. [6] showed that in the limit $Q \gg 1$ and $P_m \ll 1$, overstability is indeed possible and, therefore, the Chandrasekhar's criterion $P_r < P_m$ is not a necessary condition for overstability.

As stated above, the condition for overstability to occur has not yet been established. Moreover, to the best of our knowledge, the critical Rayleigh number R_c, the critical wavenumber a_c and the critical frequency ω_c for the onset of overstability under the proper boundary conditions have not been obtained so far. These provide us with the motivation for the present study. The main purpose of the study reported here is, therefore, to obtain the essentially exact values of R_c, a_c and ω_c for the onset of overstability and, at the same time, to get numerically a necessary and sufficient condition for overstability to occur.

2. Formulation of the problem

We consider an infinite horizontal layer of electrically conducting, viscous fluid upon which is impressed a uniform vertical magnetic induction B_0. The lower bounding surface at $z = 0$ and the upper bounding surface at $z = d$ are both rigid and are maintained at constant temperatures T_0 and T_1, respectively.

The equations governing fluid motion are given by

$$\operatorname{div}\mathbf{v} = 0 \tag{1}$$

$$\rho\left(\frac{\partial \mathbf{v}}{\partial t} + (\mathbf{v}\,\mathrm{grad})\mathbf{v}\right) = \rho\mathbf{g} - \mathrm{grad}\,p + \eta\nabla^2\mathbf{v} + \frac{1}{\mu}\mathrm{rot}\,\mathbf{B}\times\mathbf{B} \tag{2}$$

$$\rho c\left(\frac{\partial T}{\partial t} + (\mathbf{v}\,\mathrm{grad})T\right) = k\nabla^2 T \tag{3}$$

$$\rho = \rho_0\{1-\alpha(T-T_0)\} \tag{4}$$

$$\frac{\partial \mathbf{B}}{\partial t} = \mathrm{rot}(\mathbf{v}\times\mathbf{B}) + \frac{1}{\sigma\mu}\nabla^2\mathbf{B} \tag{5}$$

$$\operatorname{div}\mathbf{B} = 0 \tag{6}$$

where $\mathbf{v} = (v_x, v_y, v_z)$ is the velocity, $\mathbf{g} = (0, 0, -g)$ is the gravitational acceleration, $\mathbf{B} = (B_x, B_y, B_z)$ is the magnetic induction, ρ is the density, p is the pressure, T is the temperature, η is the dynamic viscosity, μ is the magnetic permeability, c is the specific heat, k is the thermal conductivity, α is the coefficient of volume expansion and σ is the electrical conductivity.

If the outer regions adjacent to the fluid layer are electrically non-conducting, the equations governing the magnetic induction in the regions $(-\infty < z \leqslant 0$ and $d \leqslant z < \infty)$ are

$$\nabla^2\tilde{\mathbf{B}} = 0 \tag{7}$$

$$\operatorname{div} \tilde{\mathbf{B}} = 0 \tag{8}$$

where $\tilde{\mathbf{B}} = (\tilde{B}_x, \tilde{B}_y, \tilde{B}_z)$ is the magnetic induction in the outer regions. The boundary conditions on the magnetic induction are given by

$$\frac{1}{\mu} B_x = \frac{1}{\tilde{\mu}} \tilde{B}_x \quad \text{at } z = 0, d \tag{9}$$

$$\frac{1}{\mu} B_y = \frac{1}{\tilde{\mu}} \tilde{B}_y \quad \text{at } z = 0, d \tag{10}$$

$$B_z = \tilde{B}_z \quad \text{at } z = 0, d \tag{11}$$

where $\tilde{\mu}$ is the magnetic permeability in the outer regions.

It is clear that there exist the following steady solutions (denoted by an overbar).

$$\bar{\mathbf{v}} = (0, 0, 0) \tag{12}$$

$$\bar{T} = T_0 - \beta z \tag{13}$$

$$\bar{\rho} = \rho_0 (1 + \alpha\beta z) \tag{14}$$

$$\bar{p} = p_0 - \rho_0 (z + \tfrac{1}{2}\alpha\beta z^2) g \tag{15}$$

$$\bar{\mathbf{B}} = (0, 0, B_0) \tag{16}$$

$$\bar{\tilde{\mathbf{B}}} = (0, 0, B_0) \tag{17}$$

where $\beta = (T_0 - T_1)/d$ is the adverse temperature gradient and p_0 is the pressure at $z = 0$.

Let this initial steady state be slightly perturbed. Following the usual steps of linear stability theory, we obtain

$$\left(\frac{\partial}{\partial t} - \nu\nabla^2\right)\nabla^2 v_z' = \alpha g \nabla_{\mathrm{H}}^2 T' + \frac{B_0}{\rho_0 \mu}\frac{\partial}{\partial z}\nabla^2 B_z') \tag{18}$$

$$\left(\frac{\partial}{\partial t} - \kappa\nabla^2\right) T' = \beta v_z' \tag{19}$$

$$\left(\frac{\partial}{\partial t} - \nu_{\mathrm{m}}\nabla^2\right) B_z' = B_0 \frac{\partial v_z'}{\partial z} \tag{20}$$

$$\nabla^2 \tilde{B}_z' = 0 \tag{21}$$

$$v_z' = \frac{\partial v_z'}{\partial z} = T' = 0 \quad \text{at } z = 0, d \tag{22}$$

$$B_z' = \tilde{B}_z' \quad \text{at } z = 0, d \tag{23}$$

$$\frac{1}{\mu}\frac{\partial B_z'}{\partial z} = \frac{1}{\tilde{\mu}}\frac{\partial \tilde{B}_z'}{\partial z} \quad \text{at } z = 0, d \tag{24}$$

where $\nu = \eta/\rho_0$ is the kinematic viscosity, $\kappa = k/\rho_0 c$ is the thermometric conductivity, $\nu_{\mathrm{m}} = 1/\sigma\mu$ is the magnetic viscosity, $\nabla_{\mathrm{H}}^2 = \partial^2/\partial x^2 + \partial^2/\partial y^2$ is the horizontal Laplacian and prime refers to perturbed quantities. Here the boundary conditions (24) have been obtained from equations (6) and (8) and the boundary conditions (9) and (10).

If we now introduce the following dimensionless variables:

$$(x^*, y^*, z^*) = (x/d, y/d, z/d), \quad t^* = t\nu/d^2, \quad v = v_z' d/\kappa$$
$$\theta = T'/\beta d, \quad b = B_z' \nu_{\mathrm{m}}/\kappa B_0, \quad \tilde{b} = \tilde{B}_z' \nu_{\mathrm{m}}/\kappa B_0 \tag{25}$$

equations (18)–(21) become, respectively,

$$\left(\frac{\partial}{\partial t} - \nabla^2\right)\nabla^2 v = R\nabla_{\mathrm{H}}^2 \theta + Q\frac{\partial}{\partial z}(\nabla^2 b) \tag{26}$$

$$\left(P_{\mathrm{r}}\frac{\partial}{\partial t} - \nabla^2\right)\theta = v \tag{27}$$

$$\left(P_{\mathrm{m}}\frac{\partial}{\partial t} - \nabla^2\right) b = \frac{\partial v}{\partial z} \tag{28}$$

$$\nabla^2 \tilde{b} = 0 \tag{29}$$

where $R = \alpha\beta g d^4/\nu\kappa$ is the Rayleigh number, $Q = B_0^2 d^2 \sigma/\rho_0 \nu$ is the Chandrasekhar number (the square of the Hartmann number), $P_{\mathrm{r}} = \nu/\kappa$ is the Prandtl number and $P_{\mathrm{m}} = \nu/\nu_{\mathrm{m}} = \sigma\mu\nu$ is the magnetic Prandtl number. Here the asterisks on x, y, z and t have been omitted. Similarly, the boundary conditions (22)–(24) become, respectively,

$$v = \frac{\partial v}{\partial z} = \theta = 0 \quad \text{at } z = 0, 1 \tag{30}$$

$$b = \tilde{b} \quad \text{at } z = 0, 1 \tag{31}$$

$$\varepsilon\frac{\partial b}{\partial z} = \frac{\partial \tilde{b}}{\partial z} \quad \text{at } z = 0, 1 \tag{32}$$

where $\varepsilon = \tilde{\mu}/\mu$.

If we next let

$$[v, \theta, b, \tilde{b}] = [\Phi(z), \Theta(z), \Psi(z), \tilde{\Psi}(z)] \times \exp[\lambda t + i(a_x x + a_y y)] \tag{33}$$

equations (26)–(29) become, respectively,

$$[\lambda - (D^2 - a^2)](D^2 - a^2)\Phi = -Ra^2\Theta + QD(D^2 - a^2)\Psi \tag{34}$$

$$[P_{\mathrm{r}}\lambda - (D^2 - a^2)]\Theta = \Phi \tag{35}$$

$$[P_{\mathrm{m}}\lambda - (D^2 - a^2)]\Psi = D\Phi \tag{36}$$

$$(D^2 - a^2)\tilde{\Psi} = 0 \tag{37}$$

where λ is the (complex) time constant, $a = (a_x^2 + a_y^2)^{1/2}$ is the (real) wavenumber and $D = \mathrm{d}/\mathrm{d}z$. Similarly, the boundary conditions (30)–(32) become, respectively,

$$\Phi = D\Phi = \Theta = 0 \quad \text{at } z = 0, 1 \tag{38}$$

$$\Psi = \tilde{\Psi} \quad \text{at } z = 0, 1 \tag{39}$$

$$\varepsilon D\Psi = D\tilde{\Psi} \quad \text{at } z = 0, 1. \tag{40}$$

The general solution of equation (37) is given by

$$\tilde{\Psi} = C_1\,\mathrm{e}^{az} + C_2\,\mathrm{e}^{-az}. \tag{41}$$

Since $\tilde{\Psi}$ must be finite at $z = \pm\infty$, we have

$$\Psi = C_2\,\mathrm{e}^{-az} \quad \text{for } 1 \leqslant z < \infty \tag{42}$$

$$\tilde{\Psi} = C_1\,\mathrm{e}^{az} \quad \text{for } -\infty < z \leqslant 0. \tag{43}$$

Inserting (42) and (43) into (39) and (40), and eliminating C_1 and C_2, we obtain the following boundary conditions on Ψ:

$$D\Psi + a\Psi = 0 \quad \text{at } z = 1 \tag{44}$$

$$D\Psi - a\Psi = 0 \quad \text{at } z = 0 \tag{45}$$

where we have set $\varepsilon = \tilde{\mu}/\mu = 1$, since the outer regions adjacent to the fluid layer ($-\infty < z \leqslant 0$ and $1 \leqslant z < \infty$) are assumed not to be ferromagnetic.

3. Numerical method

In order to apply the Chebyshev collocation method (see, for example, Mizushima and Saito [7]), we first introduce the new independent variable ξ defined by

$$\xi = 2z - 1 \tag{46}$$

and, furthermore, let

$$a = 2\hat{a}, \quad \omega = 4\hat{\omega}, \quad R = 16\hat{R}, \quad Q = 4\hat{Q}, \quad \Phi = 2\hat{\Phi}$$
$$\Theta = \tfrac{1}{2}\hat{\Theta}, \quad \Psi = \hat{\Psi} \quad \text{and} \quad D = 2\hat{D} = 2d/d\xi. \tag{47}$$

Then, the boundary conditions (38), (44) and (45) become

$$\Phi = D\Phi = \Theta = D\Psi \pm a\Psi = 0 \quad \text{at } \xi = \pm 1 \tag{48}$$

while equations (34)–(36) remain unchanged. Here the symbol '^' has been omitted.

We next expand Φ, Θ and Ψ as

$$\Phi = \sum_{n=1}^{N} a_n \Phi_n(\xi) \tag{49}$$

$$\Theta = \sum_{n=1}^{N} b_n \Theta_n(\xi) \tag{50}$$

$$\Psi = \sum_{n=1}^{N} c_n \Psi_n(\xi) \tag{51}$$

where

$$\Phi_n(\xi) = (1-\xi^2)^2 T_{n-1}(\xi) \tag{52}$$

$$\Theta_n(\xi) = (1-\xi^2) T_{n-1}(\xi) \tag{53}$$

$$\Psi_n(\xi) = \left(1 + \frac{2}{(n-1)^2 + a} - \xi^2\right) T_{n-1}(\xi). \tag{54}$$

Here $T_n(\xi)$ is the Chebyshev polynomial of the nth order. It should be noted here that $\Phi_n(\xi)$, $\Theta_n(\xi)$ and $\Psi_n(\xi)$ satisfy the boundary conditions (48) automatically.

Substituting (49)–(51) into equations (34)–(36) and requiring that equations (34)–(36) be satisfied at N collocation points $\xi_1, \xi_2, \ldots, \xi_N$ defined by

$$\xi_m = \cos\left(\frac{m}{N+1}\pi\right) \quad (m = 1, 2, \ldots, N) \tag{55}$$

we obtain $3N$ algebraic equations for $3N$ unknowns $a_1, a_2, \ldots, a_N, b_1, b_2, \ldots, b_N, c_1, c_2, \ldots, c_N$ of the form

$$\mathbf{EX} = \lambda \mathbf{FX} \tag{56}$$

where

$$\mathbf{X}^{\mathrm{T}} = (a_1, a_2, \ldots, a_N, b_1, b_2, \ldots, b_N, c_1, c_2, \ldots, c_N) \tag{57}$$

is the transpose of the column vector $\mathbf{X}$. The coefficient matrices $\mathbf{E}$ and $\mathbf{F}$ are of dimension $3N \times 3N$ and their explicit expressions are omitted.

For fixed values of P_r, P_m, Q, a and R, the values of λ which ensure a non-trivial solution of equation (56) can be obtained as the eigenvalues of the matrix $\mathbf{F}^{-1}\mathbf{E}$. From $3N$ eigenvalues $\lambda(1), \lambda(2), \ldots, \lambda(3N)$, the one having the largest real part ($\lambda(k)$, say), is selected. In order to obtain the neutral stability curve, the value of R for which the real part of $\lambda(k)$ vanishes must be sought. Let this value of R be denoted by R^{n}. The lowest point of R^{n} as a function of a gives the critical Rayleigh number R_c and the critical wavenumber a_c. The imaginary part of $\lambda(k)$ corresponding to R_c and a_c gives the critical frequency ω_c. If $\omega_c = 0$, the critical disturbance modes are stationary, whereas if $\omega_c \neq 0$, they are oscillatory. It is clear that the stationary mode always exists. Therefore, $R_c = R_c^{\mathrm{S}}$ when the oscillatory mode does not exist, whereas $R_c = \min(R_c^{\mathrm{S}}, R_c^{\mathrm{O}})$ when the oscillatory mode exists, where R_c^{S} and R_c^{O} are the critical Rayleigh number for the stationary and the oscillatory modes, respectively. This procedure was repeated for various values of P_r, P_m and Q.

The convergence of the Chebyshev collocation method was tested by examining the variation of R_c, a_c and ω_c with N, the number of terms retained in the expansions (49)–(51). Selected results are displayed in Table 1 for several combinations of the governing parameters. The convergence was faster in the stationary mode than in the oscillatory mode. All of the values in this table were obtained using double-precision arithmetic and confirmed using quadruple-precision arithmetic. Therefore, all of the figures in this table are considered to be significant.

4. Numerical results

The critical Rayleigh number R_c is shown in Fig. 1 as a function of the Chandrasekhar number Q for various values of the Prandtl number P_r and the magnetic Prandtl number P_m. The dashed and solid curves represent R_c^{S} and R_c^{O} for the stationary and the oscillatory modes, respectively.

The values of R_c^{S}, which is independent of P_r and P_m, is also tabulated in Table 2 as a function of Q. As in Table 1, all of the figures in this table are considered to be significant. The value of N in this table indicates the number of terms in the expansions (49)–(51) required for R_c^{S} to converge. We see from Tables 1 and 2 that the convergence of the Chebyshev collocation method becomes slower as Q increases. Numerical values of Table 2 are much more accurate than those in Table 2 of the paper by Chandrasekhar [1].

It is seen from Fig. 1 that if Q is less than a certain value, Q^*, which depends upon P_r and P_m, instability sets in a stationary mode and $R_c = R_c^{\mathrm{S}}$. However, if Q exceeds

Table 1
Selected results of convergence tests of the Chebyshev collocation method

N	R_c^S	a_c^S	ω_c	N	R_c^O	a_c^O	ω_c
$Q = 10^2$				$P_r = 10^{-2}$, $P_m = 1$, $Q = 10^2$			
4	3719.878	4.0049	0	6	3127.454	2.8845	26.570
6	3754.655	4.0121	0	8	3136.311	2.8865	26.451
8	3757.119	4.0121	0	10	3136.825	2.8866	26.442
10	3757.227	4.0120	0	12	3136.843	2.8866	26.441
12	3757.230	4.0120	0	14	3136.844	2.8866	26.441
14	3757.230	4.0120	0	16	3136.844	2.8866	26.441
$Q = 10^4$				$P = 10^{-2}$, $P_m = 1$, $Q = 10^4$			
10	124 310.8	8.6627	0	20	6362.173	3.9596	374.95
15	124 430.2	8.6645	0	25	6835.191	3.9643	374.94
20	124 501.4	8.6653	0	30	6387.303	3.9647	374.94
25	124 507.3	8.6654	0	35	6387.405	3.9647	374.94
30	124 507.6	8.6654	0	40	6387.410	3.9647	374.94
35	124 507.6	8.6654	0	45	6387.410	3.9647	374.94
$Q = 10^6$				$P_r = 10^{-2}$, $P_m = 1$, $Q = 10^6$			
50	10 320 869	18.995	0	90	38 741.48	7.4952	3482.0
60	10 321 324	18.995	0	100	38 743.54	7.4953	3482.0
70	10 321 431	18.995	0	110	38 743.82	7.4953	3482.0
80	10 321 449	18.995	0	120	38 743.85	7.4953	3482.0
90	10 321 452	18.995	0	130	38 743.86	7.4953	3482.0
100	10 321 452	18.995	0	140	38 743.86	7.4953	3482.0

Q^*, instability sets in as oscillatory mode, and $R_c = R_c^O$. To avoid confusion, the segments of the curves for R_c^O which extend above the points of intersection with the dashed curve for R_c^S are not shown.

The magnitude (Q^*) of Q at the point of transition from stationary to oscillatory mode is plotted in Fig. 2 as a function of P_m for various values of P_r. The curve markers indicate the computed points. Each curve in Fig. 2 defines the boundary between the stationary and oscillatory domains. Points below each curve represent parameter combinations (Q, P_m) for which $R_c = R_c^S$, while points above each curve are those for which $R_c = R_c^O$. Therefore, Fig. 2 gives a necessary and sufficient condition for stationary convection or overstability to occur. Comparing the criteria obtained by several investigators cited in Section 1 with our results given by Fig. 2, we see that the criteria obtained by Gibson [2] and Sherman and Ostrach [3] are correct only when Q is sufficiently large, and those obtained by Chandrasekhar [1], Gupta et al. [4] and Banerjee et al. [5] are only sufficient conditions for stationary convection to occur, whereas the criterion obtained by Kumar et al. [6] is incorrect.

The process of transition from the stationary to oscillatory mode is illustrated in Fig. 3 for $P_r = 0.01$ and $P_m = 1$. In this figure, the neutral curves for the stationary and oscillatory modes are shown for values of Q near the transition value Q^*. At $Q = 64$, the lowest point of the stationary (dashed) curve is lower than that of the oscillatory (solid) curve and, therefore, $R_c = R_c^S$. However, if Q is increased to 65, the lowest point of the stationary curve becomes higher than that of the oscillatory curve. Thus, at $Q = 65$, $R_c = R_c^O$. As Q is further increased, the stationary curve extends upward more rapidly than the oscillatory curve.

Returning to the discussion of Fig. 1, it can be seen that R_c^S increases rapidly with increasing Q, and that after transition to oscillatory mode, R_c^O increases less rapidly with increasing Q except for the case when P_m is sufficiently large. This means that, in general, the magnetic field has an inhibiting effect on the onset of instability both for the stationary and the oscillatory modes. It is also seen from Fig. 1 that R_c^O decreases with increasing P_m and increases with increasing P_r.

The critical wavenumber a_c is shown in Fig. 4 as a function of Q for various values of P_r and P_m. The dashed and solid curves represent a_c^S and a_c^O for the stationary and the oscillatory modes, respectively. The values of a_c^S, which is independent of P_r and P_m, is also tabulated in Table 2 as a function of Q. The vertical lines in Fig.

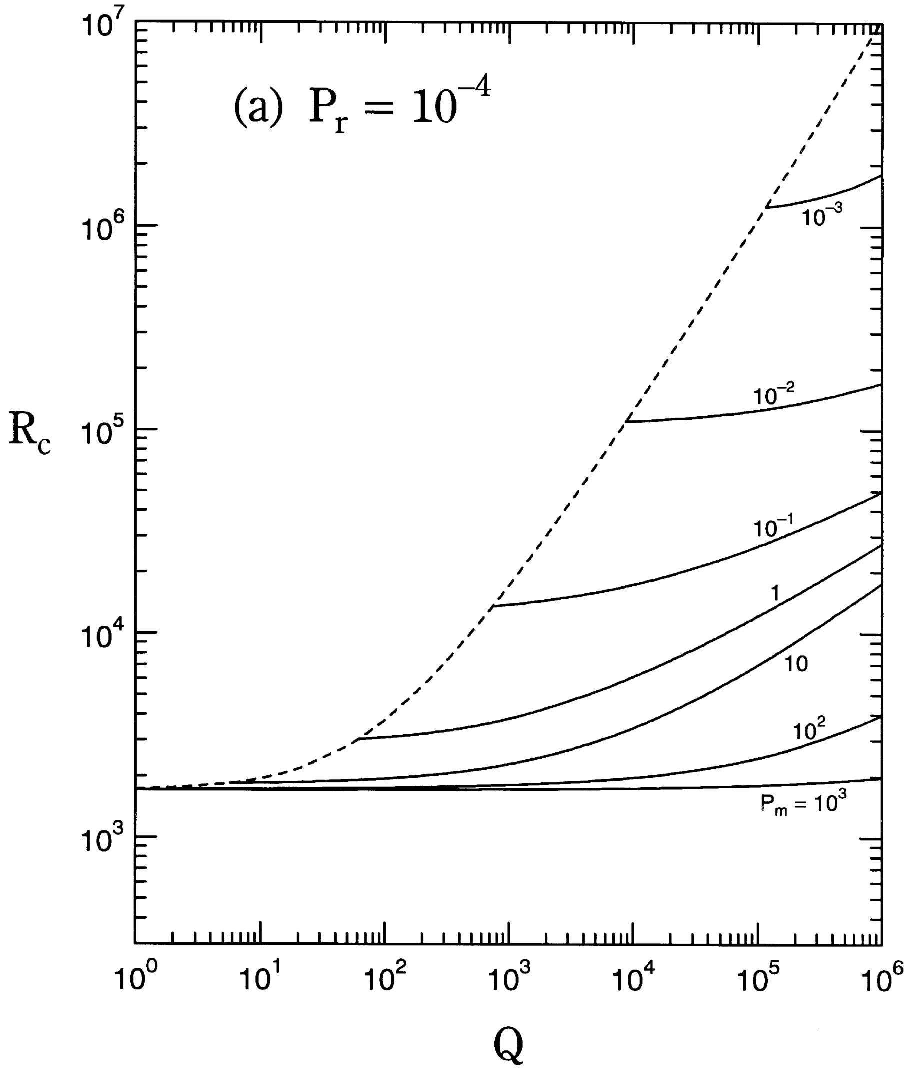

Fig. 1. Variation of the critical Rayleigh number R_c with the Chandrasekhar number Q for various values of the Prandtl number P_r and the magnetic Prandtl number P_m. - - -, stationary modes; —, oscillatory modes.

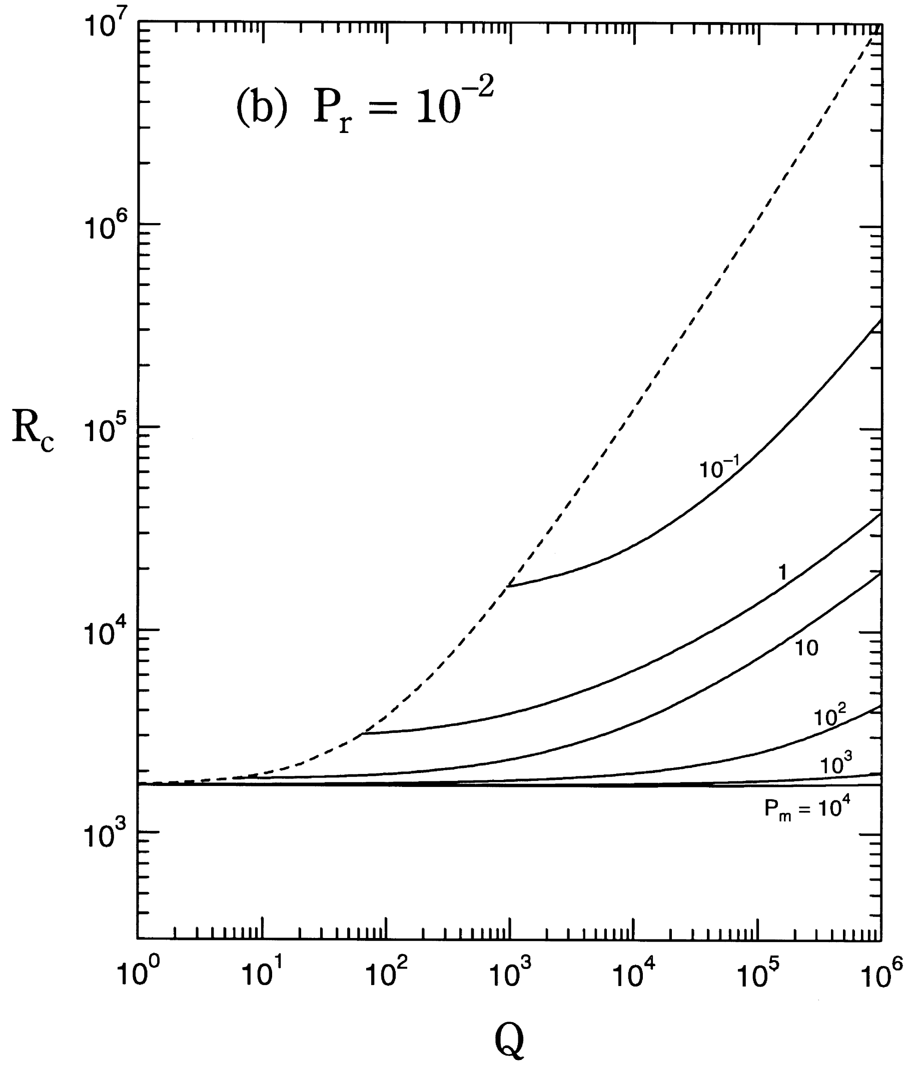

Fig. 1 (*continued*)

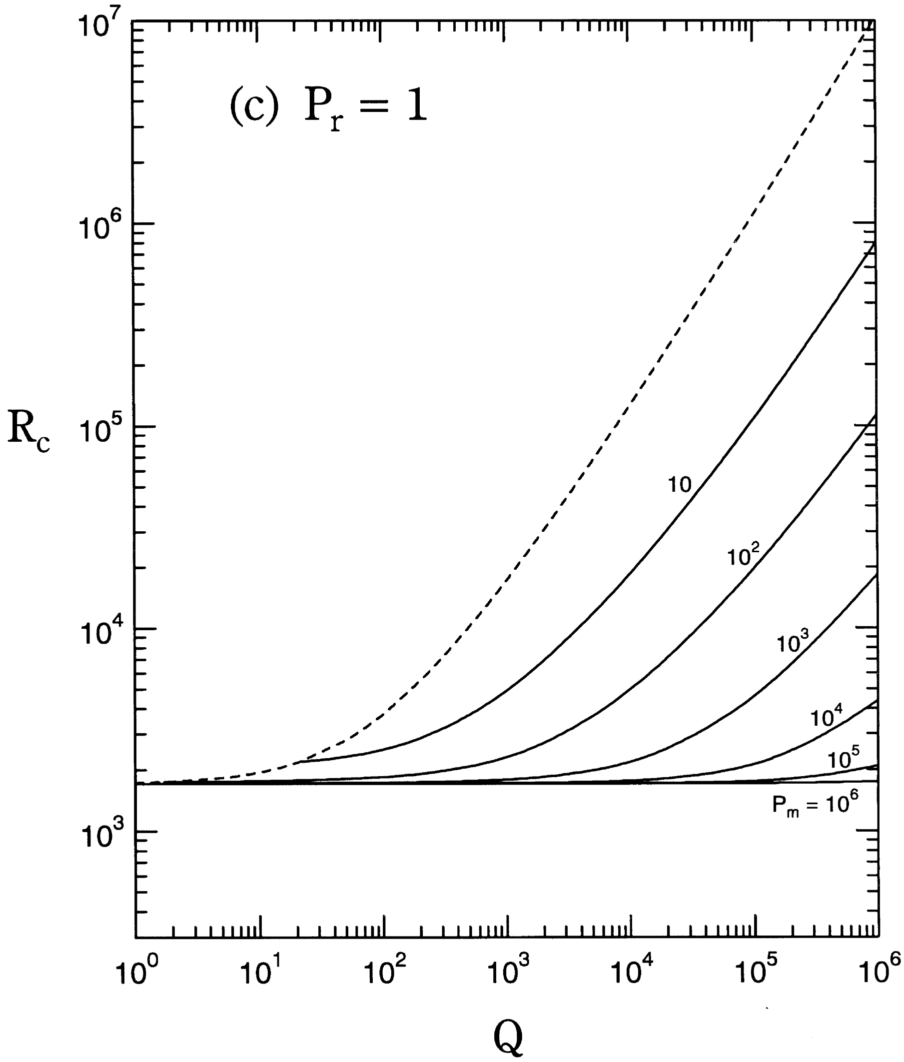

Fig. 1 (*continued*)

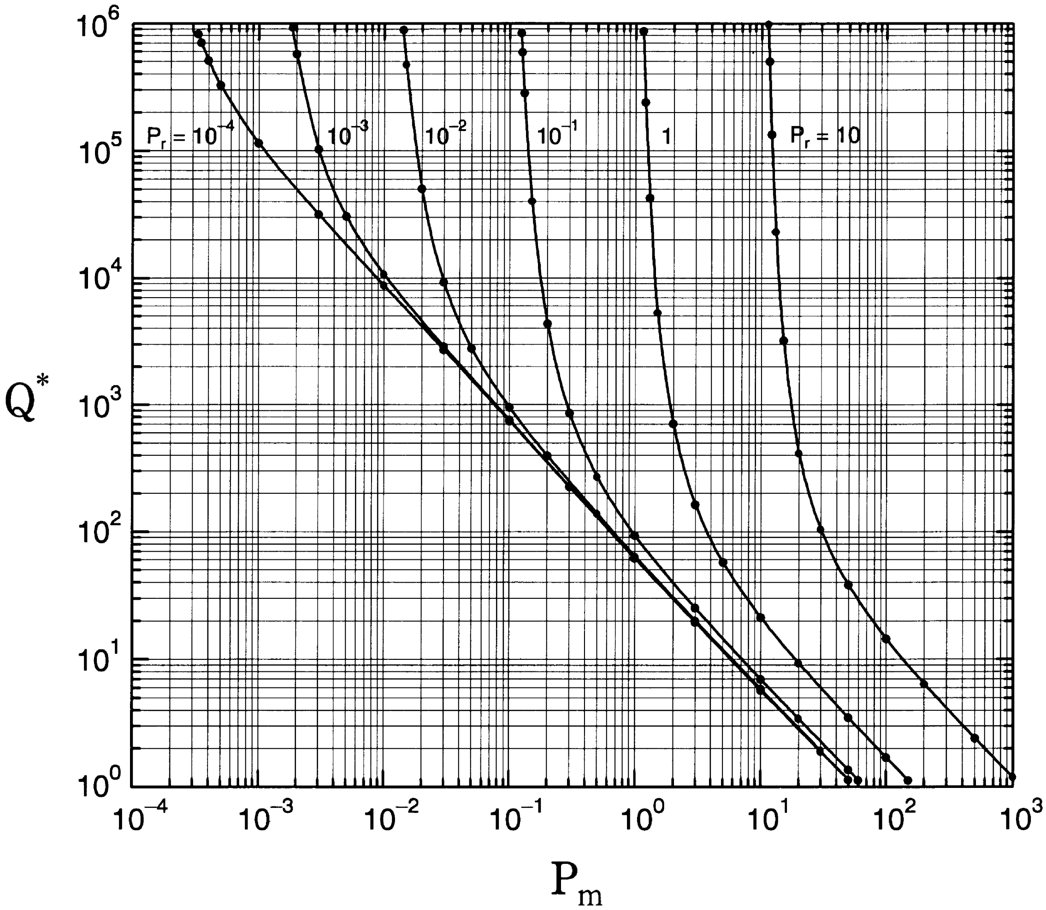

Fig. 2. The magnitude (Q^*) of the Chandrasekhar number Q at the point of transition from stationary to oscillatory mode as a function of the magnetic Prandtl number P_m for various values of the Prandtl number P_r.

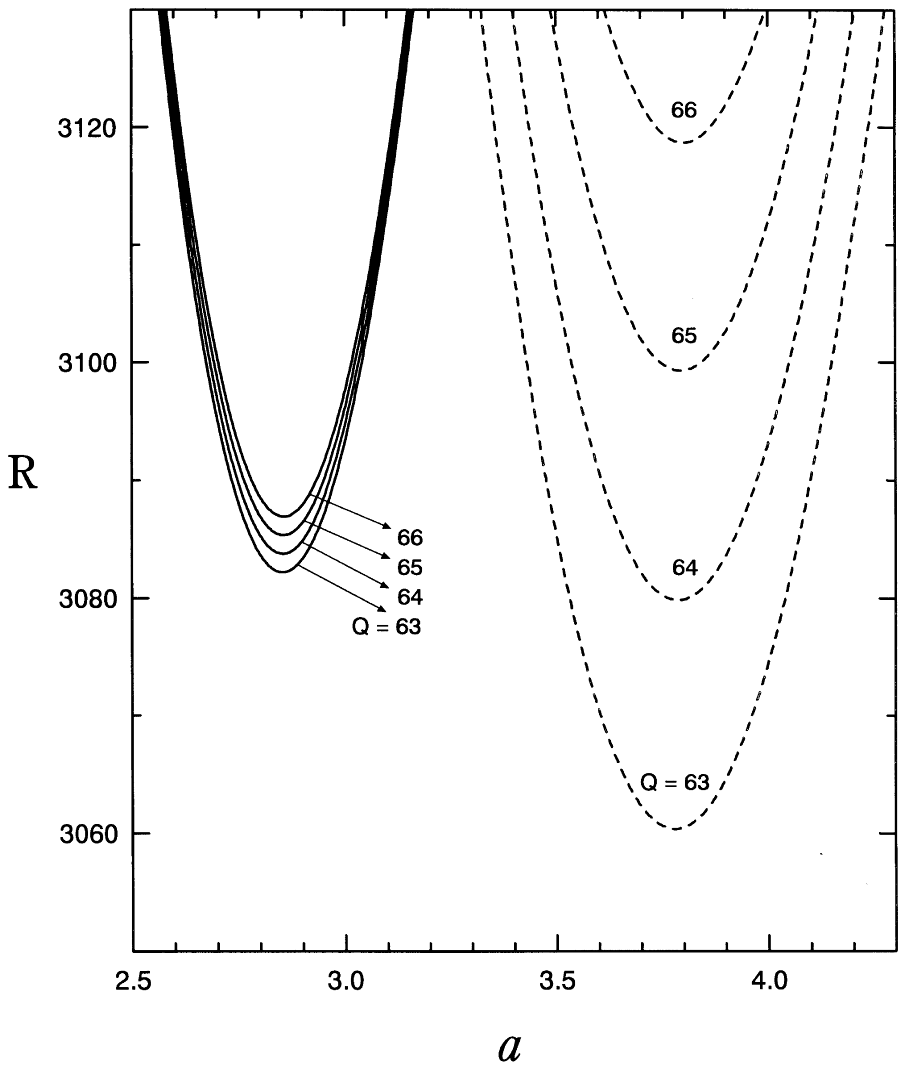

Fig. 3. Neutral stability curves for various values of Q near the point of transition from stationary to oscillatory mode when $P_r = 0.01$ and $P_m = 1$. - - -, stationary modes; —, oscillatory modes.

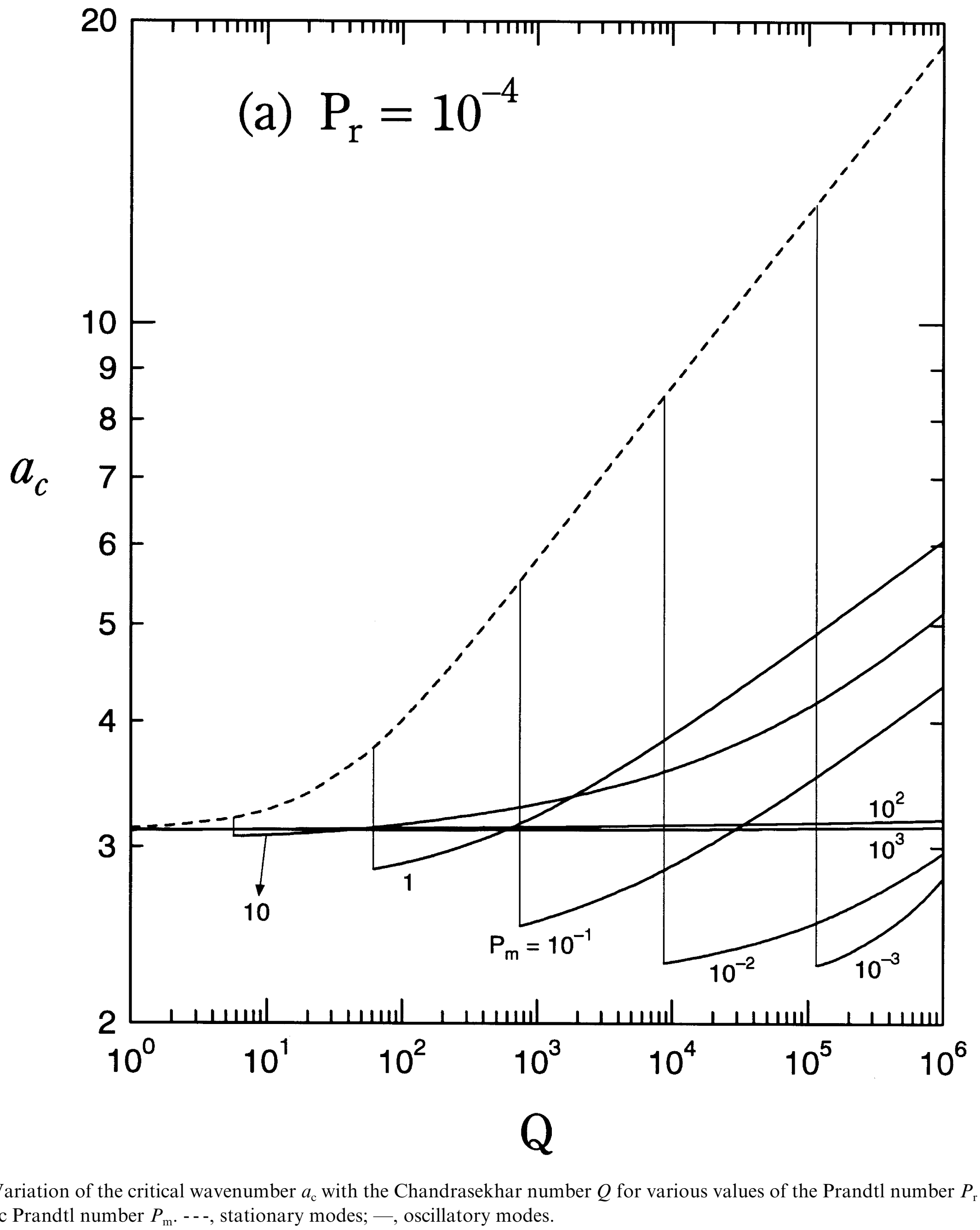

Fig. 4. Variation of the critical wavenumber a_c with the Chandrasekhar number Q for various values of the Prandtl number P_r and the magnetic Prandtl number P_m. - - -, stationary modes; —, oscillatory modes.

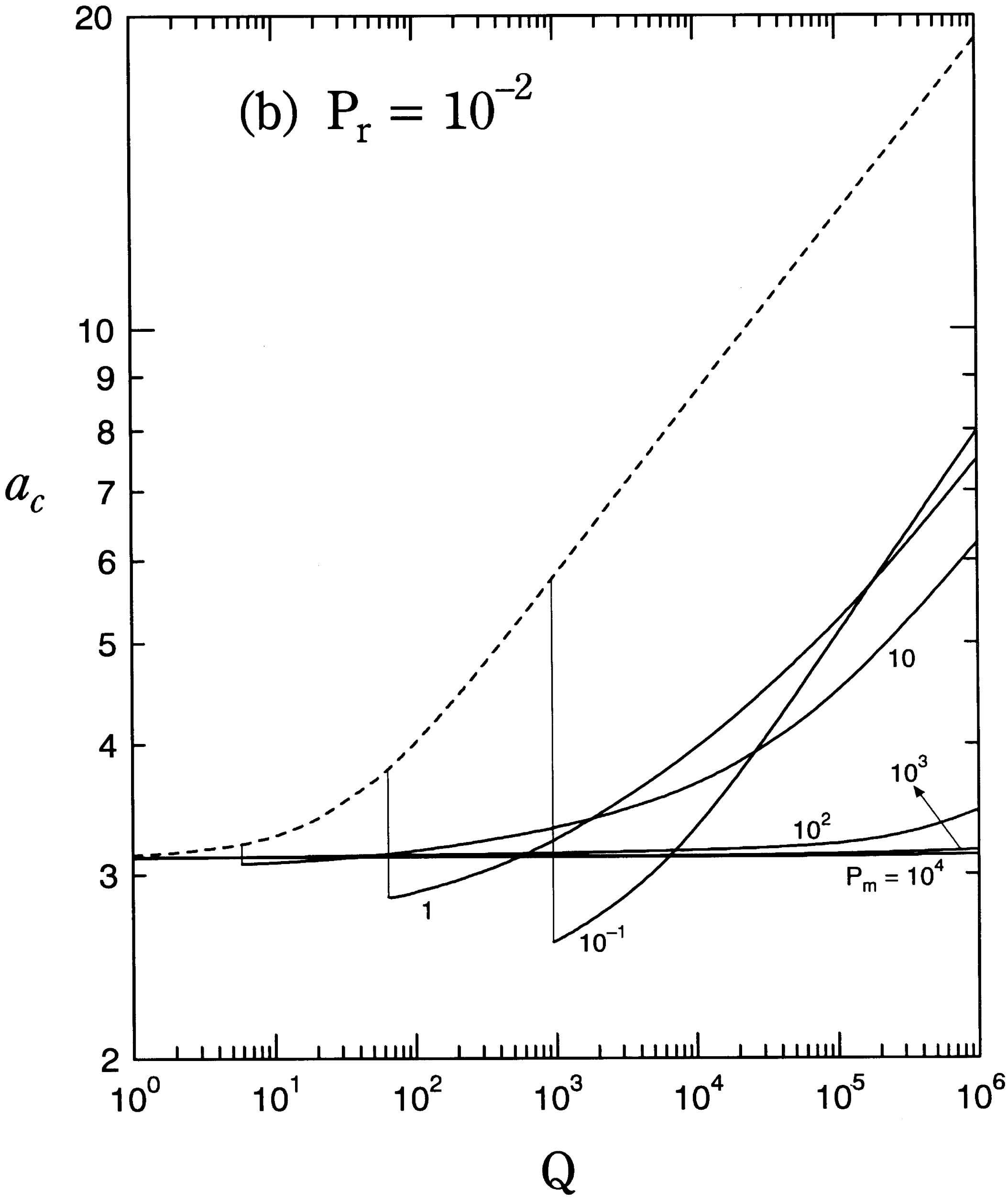

Fig. 4 (*continued*)

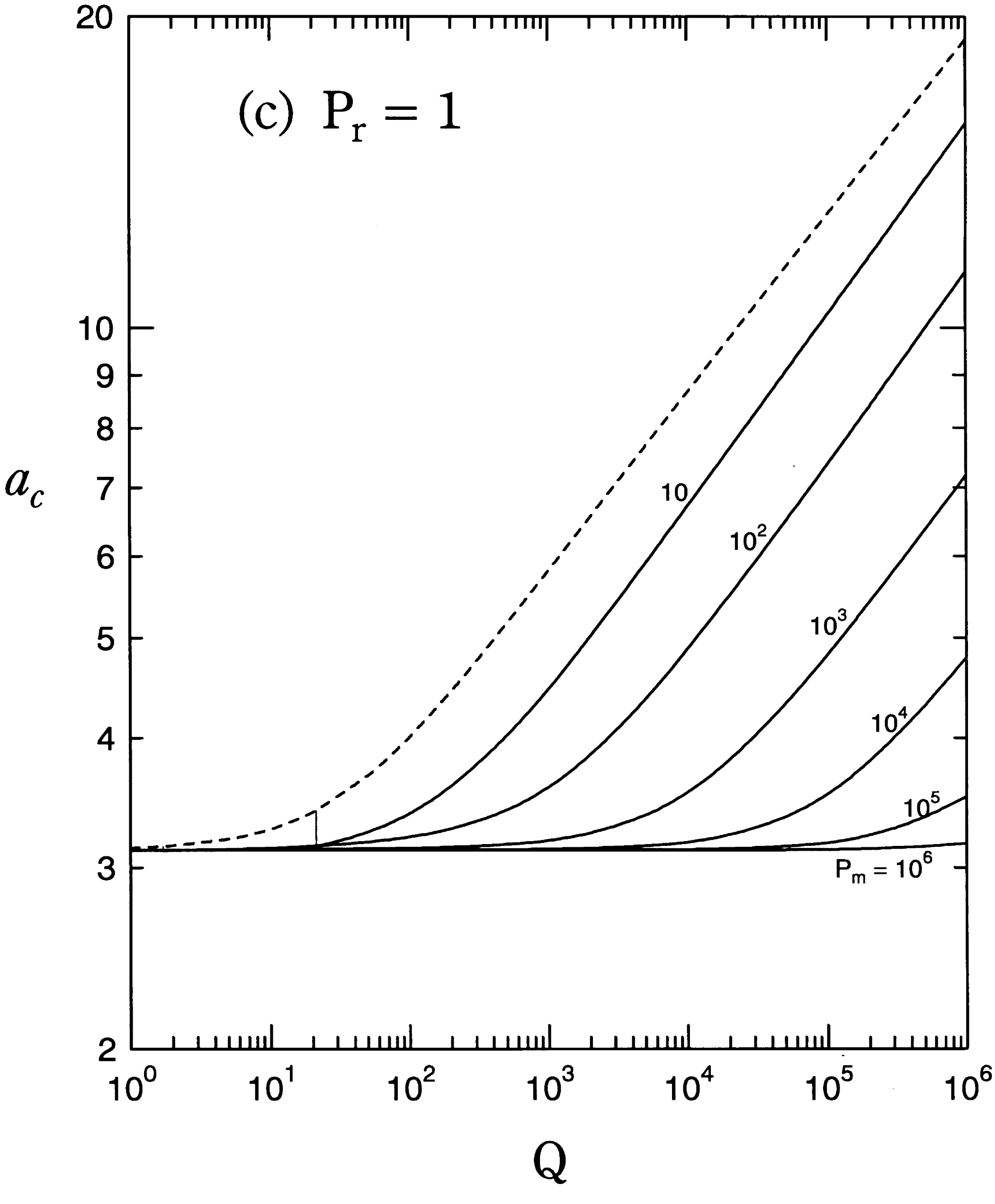

Fig. 4 (*continued*)

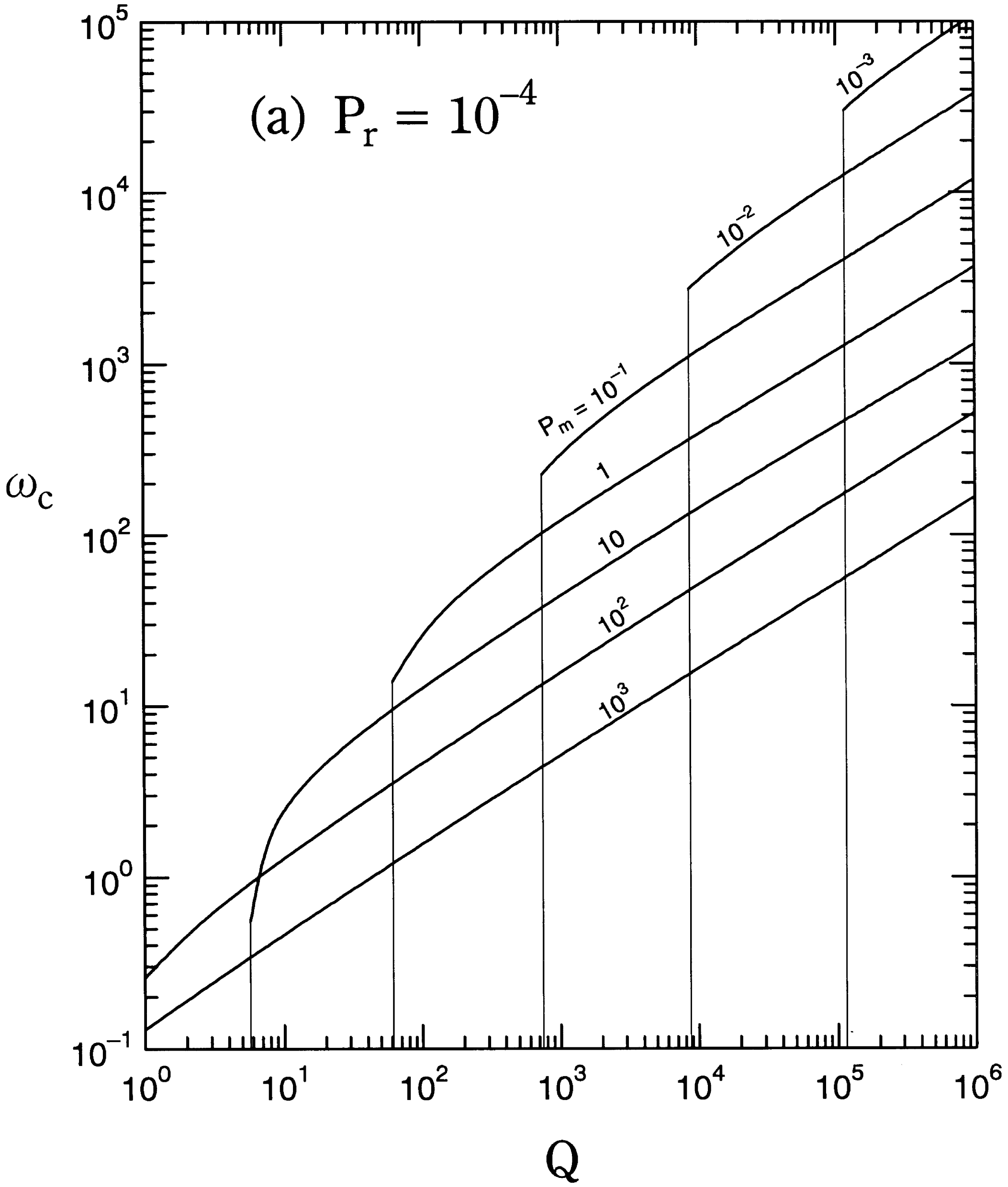

Fig. 5. Variation of the critical frequency ω_c with the Chandrasekhar number Q for various values of the Prandtl number P_r and the magnetic Prandtl number P_m.

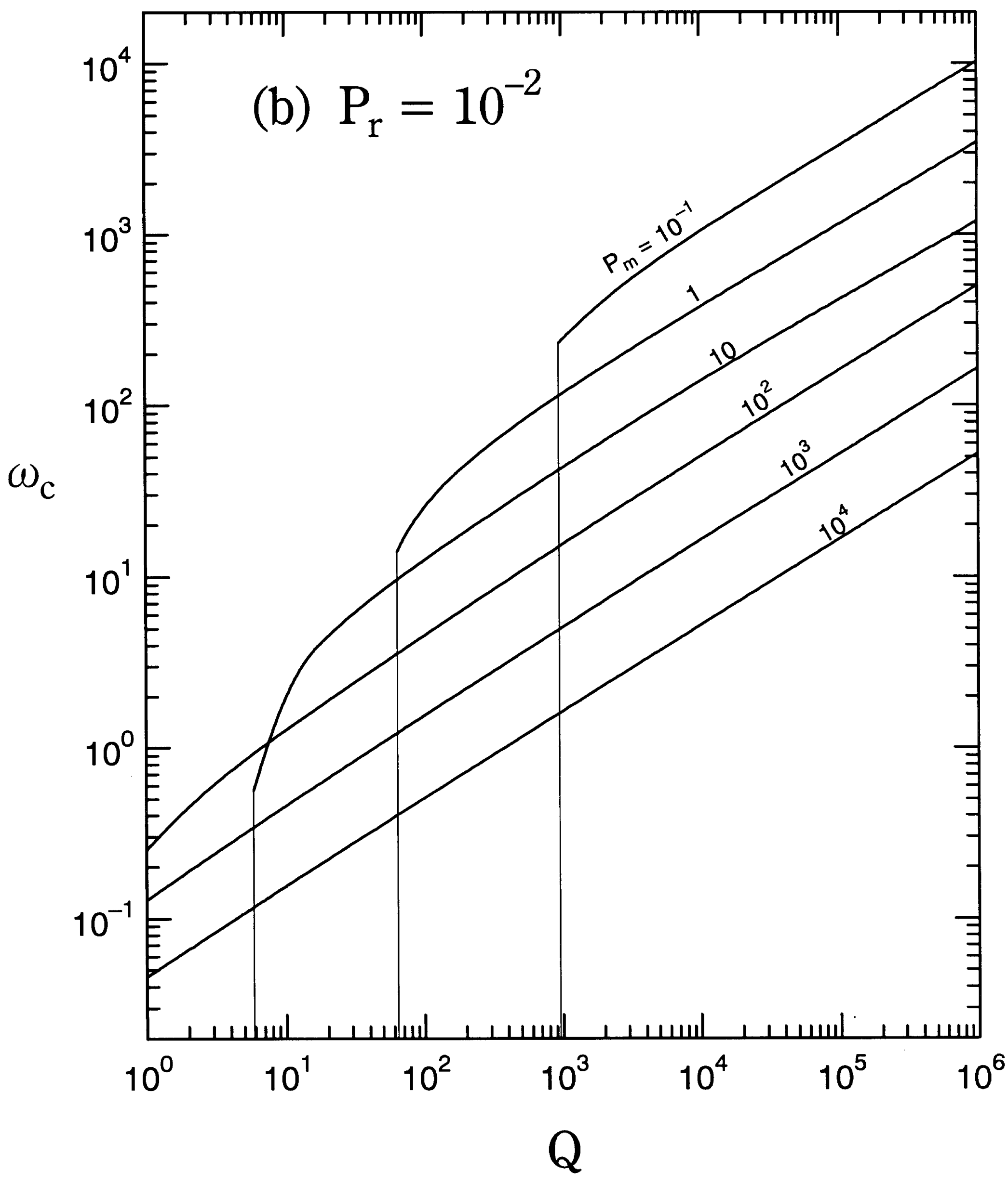

Fig. 5 (*continued*)

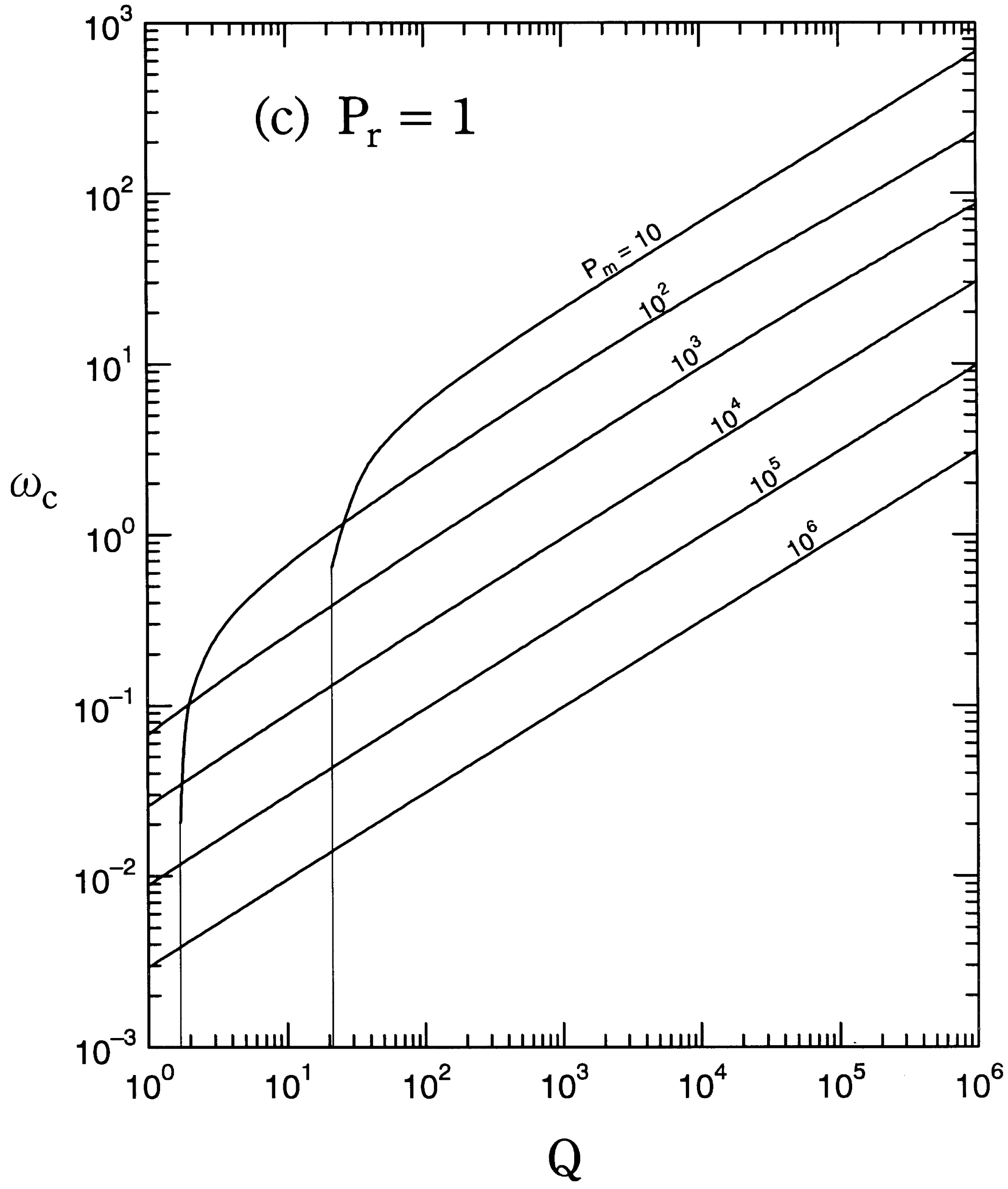

Fig. 5 (*continued*)

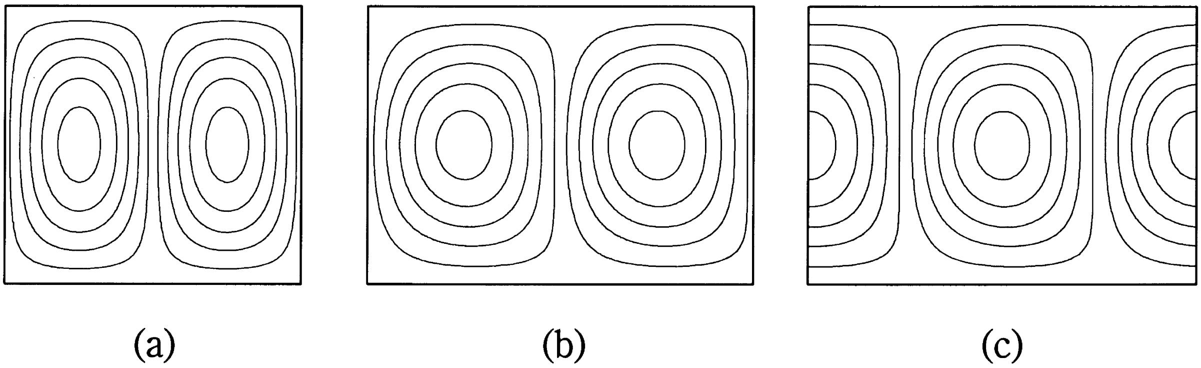

Fig. 6. Side views of streamlines at the onset of instability for the case $Q = 1000$. (a) Stationary mode, (b) oscillatory mode ($t = 0$), (c) oscillatory mode ($t = \frac{1}{4}T$).

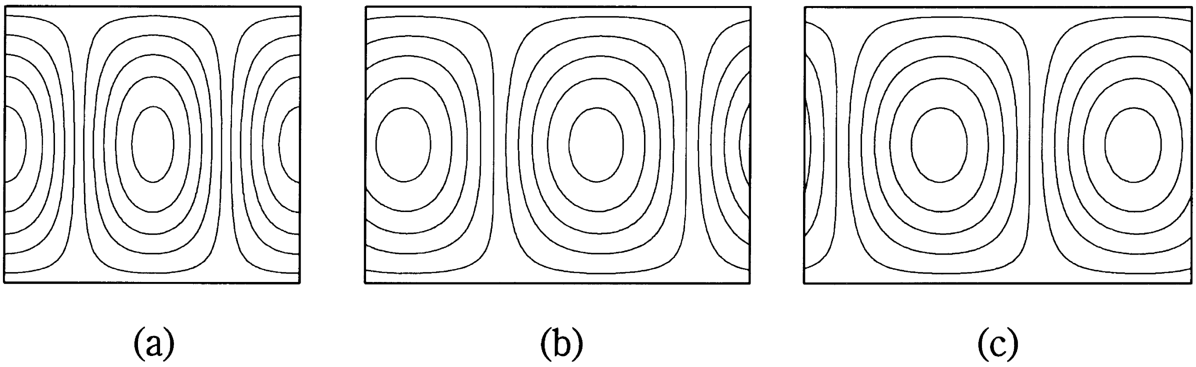

Fig. 7. Side views of isotherms at the onset of instability for the case $Q = 1000$. (a) Stationary mode, (b) oscillatory mode ($t = 0$), (c) oscillatory mode ($t = \frac{1}{4}T$).

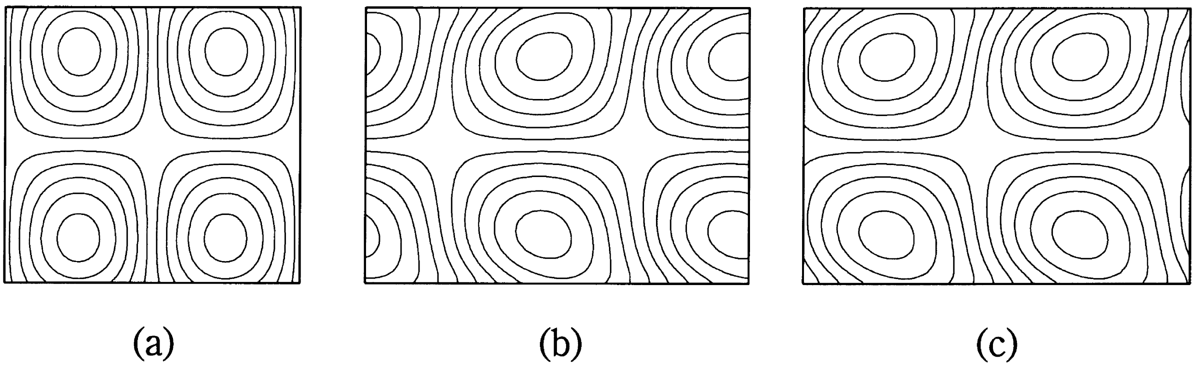

Fig. 8. Side views of magnetic lines of force at the onset of instability for the case $Q = 1000$. (a) Stationary mode, (b) oscillatory mode ($t = 0$), (c) oscillatory mode ($t = \frac{1}{4}T$).

Table 2
Variation of the critical Rayleigh number R_c^S and the critical wavenumber a_c^S for the onset of stationary convection with the Chandrasekhar number Q

Q	R_c^S	a_c^S	N
0	1707.762	3.1163	10
1	1732.210	3.1326	10
2	1756.500	3.1485	10
5	1828.479	3.1944	10
10	1945.746	3.2653	10
20	2171.786	3.3903	10
50	2802.006	3.6792	15
100	3757.230	4.0120	15
200	5488.533	4.4458	15
500	10 109.766	5.1648	20
1000	17 102.84	5.8140	20
2000	30 124.76	6.5552	25
5000	66 618.78	7.6854	30
10 000	124 507.6	8.6654	30
20 000	236 395.5	9.7654	35
50 000	561 671.4	11.4271	50
100 000	1 091 807.9	12.8618	60
200 000	2 135 956	14.470	60
500 000	5 224 694	16.898	70
1 000 000	10 321 452	18.995	90

N is the number of terms in the expansions (49)–(51) for R_c^S and a_c^S to converge.

4 represent the discontinuous changes in a_c due to the transition from stationary to oscillatory mode. We see from Fig. 4 that both a_c^S and a_c^O are increasing functions of Q, while the dependence of a_c^O on P_r and P_m is complicated.

Additional information regarding the nature of the oscillatory instability can be obtained from Fig. 5, which shows the variation of the critical frequency ω_c with Q for various values of P_r and P_m. The vertical lines represent the discontinuous changes in ω_c due to the transition from stationary ($\omega_c = 0$) to oscillatory ($\omega_c \neq 0$) mode. We see from Fig. 5 that ω_c is an increasing function of Q, P_r and P_m.

It is finally concluded from Figs 1 and 2 that under most terrestrial conditions ($P_r > P_m$), instability sets in as stationary convection. In fact, experiments by Nakagawa [8, 9] for a horizontal layer of mercury show no evidence of overstability. Under astrophysical conditions ($P_r \ll P_m$), however, overstability will be possible. It is also concluded from Figs 1 and 4 that as P_m becomes sufficiently large, R_c^O and a_c^O become nearly independent of Q, as far as $Q \leqslant 10^6$. This means that under astrophysical conditions ($P_r \ll P_m$), the magnetic field has almost no effect on buoyancy driven instability except for its frequency.

In closing this section, side views of streamlines, isotherms and magnetic lines of force at the onset of instability are shown in Figs 6, 7 and 8, respectively, for the case $Q = 1000$. The other parameter values taken in oscillatory modes are $P_r = 1$ and $P_m = 10$. The region shown is $0 \leqslant x \leqslant 2\pi/a_c$ and $0 \leqslant z \leqslant 1$. In the captions of these figures, T denotes the period of oscillation. We see from Figs 6, 7 and 8 that when disturbances are stationary, streamlines, isotherms and magnetic lines of force are symmetric with respect to a vertical centre plane of a cell, whereas when disturbances are oscillatory, they are not symmetric.

References

[1] S. Chandrasekhar, On the inhibition of convection by a magnetic field, Philosophical Magazine 43 (1952) 501–532.
[2] R.D. Gibson, Overstability in the magnetohydrodynamic Bénard problem at large Hartmann numbers, Proceedings of the Cambridge Philosophical Society 62 (1966) 287–299.
[3] M. Sherman, S. Ostrach, On the principle of exchange of stabilities for the magnetohydrodynamic thermal stability problem in completely confined fluids, Journal of Fluid Mechanics 24 (1966) 661–671.
[4] J.R. Gupta, S.K. Sood, U.D. Bhardwaj, On Rayleigh–Bénard convection with rotation and magnetic field, Journal of Applied Mathematics and Physics 35 (1984) 252–256.
[5] M.B. Banerjee, J.R. Gupta, R.C. Shandil, S.K. Sood, On the principle of exchange of stabilities in the magnetohydrodynamic simple Benard problem, Journal of Mathematical Analysis and Applications 108 (1985) 216–222.
[6] K. Kumar, J.K. Bhattacharjee, K. Banerjee, Overstability in magnetohydrodynamic convection revisited, Physics of Fluids 29 (1986) 4032–4032.
[7] J. Mizushima, Y. Saito, Equilibrium characteristics of the secondary convection in a vertical fluid layer between two flat plates, Fluid Dynamics Research 2 (1987) 183–191.
[8] Y. Nakagawa, An experiment on the inhibition of thermal convection by a magnetic field, Nature 175 (1955) 417–419.
[9] Y. Nakagawa, Experiments on the inhibition of thermal convection by a magnetic field, Proceedings of the Royal Society (London) A240 (1957) 108–113.